Available online at www.sciencedirect.com

ScienceDirect

Procedia Structural Integrity 12 (2018) 122–129

Structural Integrity Procedia

www.elsevier.com/locate/procedia

AIAS 2018 International Conference on Stress Analysis

3D vibration measurements by a virtual-stereo-camera system based on a single low frame rate camera

Sandro Barone[a], Paolo Neri[a,]*, Alessandro Paoli[a], Armando Viviano Razionale[a]

[a]*University of Pisa. Department of Civil and Industrial Engineering, Mechanical Division. Largo L. Lazzarino 1, 56122 Pisa, Italy*

Abstract

A 3D full-field optical system for high frequency vibration measurement is proposed. The system is composed of a single low-frame-rate camera and two planar mirrors. This compact optical setup overcomes the typical drawback of capturing synchronous acquisitions in the case of a camera pair. Moreover, planar mirrors allow for the use of the classical pinhole model and, thus, conventional stereo-calibration techniques. The use of a low-frame-rate camera provides on the one hand a high-resolution sensor with a relatively low-cost hardware but imposes, on the other, the adoption of a down-sampling approach, which is applicable only when a single (known) sinusoidal load is applied to the structure. The effectiveness of the proposed setup has been verified by the 3D vibration measurement of two different targets up to a frequency of 1 kHz, corresponding to a displacement amplitude of 0.01 mm.

Keywords: Reverse engineering; digital image correlation; single low-speed camera; down-sampling approach.

1. Introduction and background

Several industrial applications are characterized by vibrational loading, which may cause fretting issues, noise increment, efficiency losses and fatigue failures. The dynamic characterization of rotating machines (e.g. turbines and compressors) is usually performed through Experimental Modal Analysis (EMA) and experimental Harmonic

* Corresponding author. Tel.: +39-050 2218019; fax:+39-050 2218019.
E-mail address: paolo.neri@dici.unipi.it

10.1016/j.prostr.2018.11.101

Response Analysis (HRA) (Bertini et al., 2014; Kammerer and Abhari, 2009). Since contact methods may influence the structures response, non-contact techniques were developed. Among these, Laser Doppler Vibrometry (LDV) is one of the most commonly adopted (Lezhin et al., 2017). However, conventional LDV sensors allow 1-D single point measurements, thus resulting in highly time-consuming tests. This issue can be mitigated by adopting robotic arms to automatize the test (Bertini et al., 2017), or by using continuous scanning LDV (Giuliani et al., 2013; Halkon and Rothberg, 2006). Anyway, these techniques only provide mono-dimensional measurements, being limited in measurement direction and also presenting positioning issues when dealing with complex geometries.

Vision measurement systems were then developed in several engineering fields to overcome the above described issues (Sutton, 2013). Vision systems allow for fast full-field measurements which rely in relatively low-cost hardware. Stereo Digital Image Correlation (stereo-DIC) is one of the most promising techniques in this scenario (Beberniss and Ehrhardt, 2017). The working principle of stereo-DIC is based on the use of a stereo camera pair to acquire two synchronous images of the vibrating object from two different perspectives. If the target surface is prepared with a high-contrast speckle pattern, it is then possible to reconstruct the surface 3D displacement over time by applying the stereo-DIC algorithm. Generally, a pair of synchronized high-speed cameras is adopted to measure high-frequency vibrations (Helfrick et al., 2011; Reu et al., 2017), having a high cost and presenting synchronization problems. Many researchers overcome this issue by designing compact pseudo-stereo systems setups based on a single camera and additional optical devices, such as biprisms, diffraction gratings or a set of planar mirrors (Pan et al., 2018). All these configurations split the camera sensor in two or more regions where the target is imaged from different perspectives, thus avoiding the need of camera synchronization. Anyway, most of the applications exploit a high-speed camera in order to fulfill the Nyquist-Shannon theorem requirements in dynamic regimes (Pankow et al., 2010; Yu and Pan, 2017). This extends the maximum measurable frequency, but reduces the camera resolution (and, thus, the acquisition accuracy) with a drastic cost increase.

In this paper, two planar mirrors were placed in front of a low-frame-rate camera to obtain a pseudo-stereo DIC system (Gluckman and Nayar, 2001). This allowed to achieve two main goals: defining a compact optical setup and determining a low cost high-resolution system. Blur images were avoided by adopting a short exposure time, and a down-sampling approach (Endo et al., 2015) was adopted to overcome the Nyquist-Shannon frequency limitation. Thus, the proposed system can measure only vibrations characterized by a single known harmonic component. The Non-Harmonic Fourier Analysis (NHFA) was used to obtain an accurate reconstruction of the down-sampled signal frequency, amplitude and phase (Neri, 2017). The developed system was validated by measuring a cantilever plate excited with an electrodynamic shaker with a single-frequency sinusoidal force. An accelerometer was used to compare the vibration amplitude with a frequency up to 1 kHz (even if the maximum camera frame rate is 178 fps). Finally, the proposed method was experienced in the vibration measurement of a turbine blade, which represents a relevant industrial application.

2. Measurement principles

The aim of this research activity is to carry out 3D high frequency vibration measurements without using high speed cameras. Two main issues arise in this scenario: the ratio between the sample frequency and the measured signal is lower than two (not respecting the Nyquist-Shannon theorem) and the stereo matching problem between left and right picture must be solved. This section exposes how these problems were faced by using relatively low-cost hardware.

2.1. Down-sampling strategy

It is well known that, in general, a sampling frequency which is at least double of the measured signal frequency is needed to avoid aliasing phenomena. Anyway, this condition can be relaxed if the acquired signal is characterized by a single sinusoidal component having a known frequency. Recent works demonstrated that the amplitude and the actual frequency of the down-sampled signal may be retrieved by using NHFA, which mainly consists in a least square fit of the down-sampled signal with a sinusoidal function (Barone et al., 2017). Moreover, the acquisition sampling frequency can be properly chosen to ensure that a full vibration period is measured. Being n_s the number of samples to be acquired, f_v the vibration frequency and $T_v = 1/f_v$ the vibration period, it is possible to compute the time interval Δt between the theoretically desired samples as $\Delta t = T_v/n_s$. The theoretical sampling frequency should then be equal

to $f_{s,th} = 1/\Delta t$, which allows to acquire points corresponding to $S(t_i)$ and $S(t_i+\Delta t)$, being $S(t)$ the signal amplitude at time t. However, $f_{s,th}$, in general, may be higher than the maximum frame rate available for low speed cameras. In this case, it is possible to use the periodicity property of the signal to relax the constraint. Indeed, for signals having a single harmonic component, it is possible to state that $S(t_i+\Delta t) = S(t_i+\Delta t+kT_v)$, where k is an integer value, which can be arbitrarily chosen without any restriction. Thus, the actual time interval between acquisitions becomes $\Delta t_d = \Delta t+kT_v$ and the sampling frequency f_s can be defined as $f_s = f_v\ n_s\ /(1+k)$. It is worth noting that the sampling frequency f_s decreases if a high value of k is chosen, thus the camera sampling frequency does not represent a limitation with the proposed approach. On the other hand, high frequency vibrating targets still are challenging to be acquired since a blur image would be obtained if the exposure time E is close to T_v. To overcome this issue, a digital camera with a shutter time much shorter than T_v ($E < T_v/50$) was used. Finally, the actual amplitude and frequency of the measured vibration is computed with the NHFA algorithm. It is worth noting that the NHFA algorithm does not require a specific f_s to be adopted during the acquisition. Anyway, in the following, the sampling frequency as expressed above was used to ensure the complete description of at least one vibration period.

2.2. Digital Image Correlation strategy

In the present paper, a virtual-stereo vision system was assembled to achieve 3D surface measurements. The stereo triangulation principle was used to obtain the three-dimensional coordinates of the point cloud representing the target surface starting from the two 2D acquisitions. More precisely, a virtual stereo camera setup was developed by exploiting two planar mirrors with different orientations with respect to the camera. More details about the optical setup are provided in the following section. Regardless the optical configuration, stereo triangulation is based on the solution of the stereo matching problem, i.e. defining a map function that match corresponding points on the two camera image planes. In this work, this problem was solved by exploiting a 2D DIC algorithm (Eberl, 2010). In practice, a random speckle pattern was sprayed on the target, and a first acquisition of the stationary target was carried out with the optical system. A DIC grid was defined on the left image ($grid_{L,0}$) and the 2D DIC algorithm was exploited to find the grid of the corresponding points on the right image ($grid_{R,0}$). This allowed to compute the 3D coordinates of the grid points corresponding to the surface of the measured object by conventional stereo-triangulation. Subsequently, any time that a displacement field was applied to the target, another acquisition could be carried out. It was not required to repeat the DIC analysis between left and right image since the stereo matching problem was solved in the previous step. Indeed, for the i-th acquisition, the points belonging to $grid_{L,0}$ and $grid_{R,0}$ were traced during the displacement by separately using the 2D DIC algorithm on left and right images. This allows the definition of two grids, $grid_{L,i}$ and $grid_{R,i}$, which represent the location of the measurement points on left and right image planes. It is worth noting that the points in $grid_{L,0}$ correspond to the points in $grid_{R,0}$, thus the points of $grid_{L,i}$ correspond to the points of $grid_{R,i}$. This means that the stereo triangulation of $grid_{L,i}$ and $grid_{R,i}$ produces the 3D point cloud corresponding to the deformed object at the i-th deformation stage. This procedure is schematized in Fig. 1. The stereo matching is solved only once on image 0, and then the same grids are used to track the deformation in the i-th image, thus reducing computational time, which may be not negligible when i increases.

3. Optical system

3.1. Hardware setup

The stereo vision system was obtained by assembling two rectangular planar mirrors (30 × 30 mm), placed in front of a single camera (TREX, Visionlink, maximum resolution 2024 × 2024, maximum frame rate 178 Hz, minimum shutter time 2 μs) with a fixed angle. A pseudo-stereo setup is then defined, since the target object is imaged from two different views even using a single camera. Figure 2 shows the experimental setup during the acquisition process of a target surface. The use of planar mirrors theoretically does not introduce any image distortion. The stereo system calibration can then be performed with conventional procedures, such as the one implemented in the Matlab Camera Calibration Toolbox, which is based on the acquisition of a chessboard placed in several positions in front of the camera system (Bouguet, 2015).

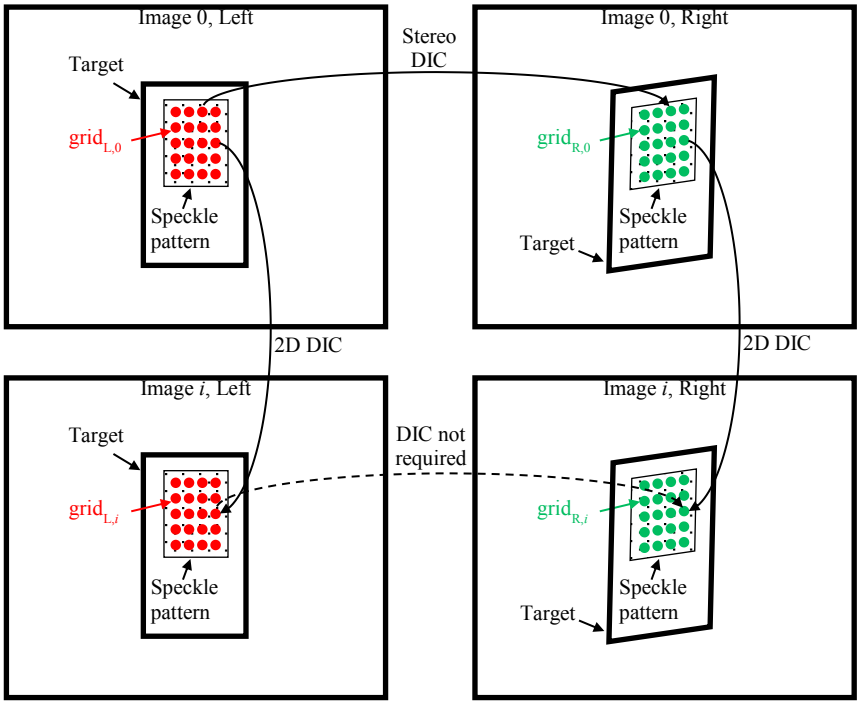

Fig. 1. Schematic representation of the use of 2D DIC for 3D shape reconstruction.

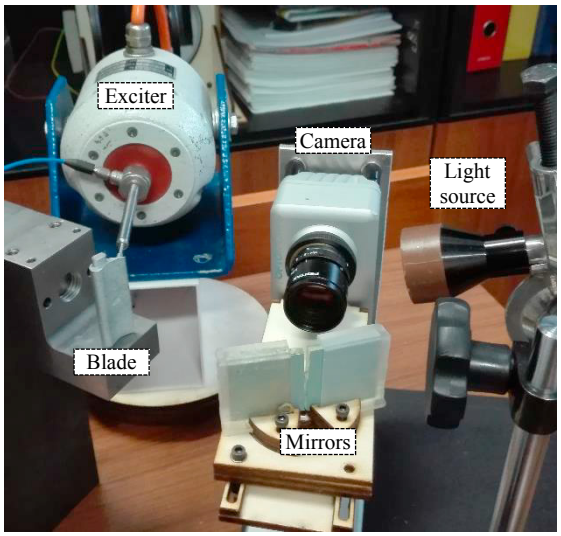

Fig. 2. Experimental setup during the acquisition process of a target surface

3.2. System characterization

The described unconventional optical setup was characterized in terms of measurement noise and accuracy by acquiring a static planar surface with a speckle pattern sprayed on it. The proposed DIC strategy was adopted to solve the stereo matching problem. A point cloud corresponding to the acquired surface was then obtained by exploiting the stereo-triangulation principle. The point cloud was used to compute the best fit plane, obtaining a standard deviation of 0.028 mm. This was considered a well reasonable result, which is perfectly comparable with typical optical setups

outcomes, confirming that the conventional calibration procedure is still applicable to the proposed bi-mirror configuration.

4. Experimental tests

The proposed procedure was experimentally tested by performing vibration measurements on two different targets. Firstly, a rectangular area of an aluminum cantilever beam was measured and compared to the results obtained by a triaxial accelerometer (Dytran Intruments Inc., model 3133A1). Then, a turbine blade with a curved surface was measured through the DIC system to show the application of the methodology to a real industrial object. In both cases, an electrodynamic shaker was used to apply the sinusoidal loading at the desired frequency through a stinger.

4.1. Validation

A cantilever beam was obtained by screwing a rectangular aluminum sheet (70 × 150 × 3 mm) to a basement. The DIC random speckle pattern was sprayed on the front surface of the target with black paint on a white paint background (measurement area: 20 × 40 mm). The shaker was then applied to the top-left corner of the beam, in order to excite both torsional and bending modes. An accelerometer was attached to the back surface of the beam, in correspondence of the top-right corner of the DIC pattern, in order to measure both torsional and bending modes. The tests were performed for increasing vibration frequencies, in the range 150-920 Hz. It is worth noting that the maximum camera frame rate was 178 fps, which corresponds to a maximum measurable frequency of 89 Hz if the Nyquist-Shannon theorem is to be respected. Figure 3(a) represents the displacement map for the 150 Hz excitation computed with the frame corresponding to the maximum of the signal. The displacements of the points corresponding to the application area of the accelerometer (i.e. red box in Fig. 3(a)) were then extracted and plotted over time, as shown in Fig. 3(b).

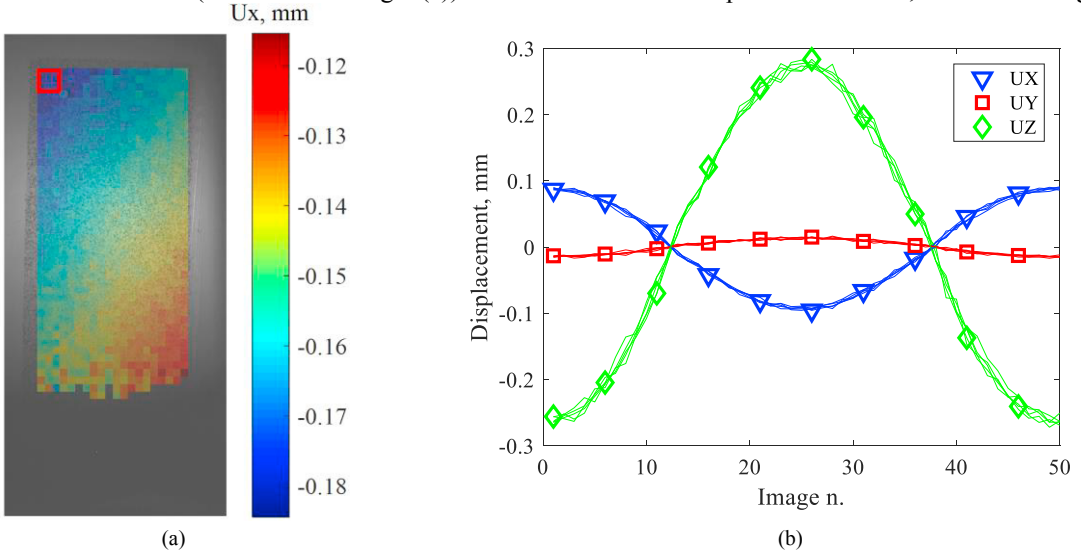

(a) (b)

Fig. 3. DIC results for the validation specimen: (a) full field displacement at maximum deformation and (b) displacement over time of the selected points.

Three displacement components are obviously available, since the stereo system can detect 3D displacements. This measurement was compared with the accelerometer signal. Firstly, the displacement (d) was computed from the acceleration (a) by using the formula: $d = a/\omega^2$, being ω the vibration angular frequency in rad/s. Anyway, the reference frame of the accelerometer was not coincident with the camera reference frame, so that the three displacement components could not be directly compared with DIC results. The magnitude of the displacement was then computed to avoid any reference frame ambiguity. It is important to highlight that the accelerometer was acquired with a sampling frequency of 10 kHz, thus amplitude and frequency information could be directly obtained through

traditional Fourier analysis. Anyway, to achieve a graphical comparison, the accelerometer signal was virtually down-sampled with the same f_s of the camera. The comparison between the accelerometer signal, the DIC measured signal and the NHFA elaboration of the DIC signal is reported in Fig. 4(a), which shows the mean value of the displacement values measured in correspondence of the accelerometer application area. A relative error of 2% was obtained between the accelerometer amplitude and the NHFA amplitude, proving the effectiveness of the method. Also, the noise level in this application appears low if compared to the signal amplitude which is in the order of 0.4 mm.

The measurements were then repeated at higher frequencies to assess the capability of the system. Higher frequencies cause the object to move faster, thus blur phenomena may occur. Moreover, higher frequencies generally cause smaller displacements. Figure 4(b) shows the results obtained at 920 Hz, confirming that the amplitude decreases when the frequency increases. From Fig. 4(b), it is also possible to note that for a vibration frequency of 920 Hz the amplitude is lower than 0.015 mm. However, the relative error between stereo-DIC and the accelerometer is about 9%, thus confirming that the system is still able to measure such small high-frequency vibrations.

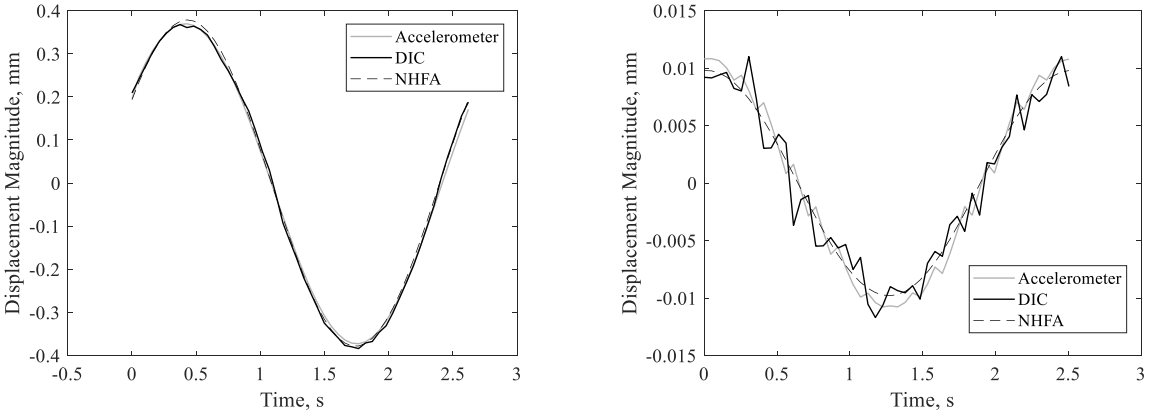

Fig. 4. Comparison between vibration magnitudes of stereo-DIC and accelerometer measurements obtained for (a) 150 Hz, (d) 920 Hz frequency values.

4.2. Industrial application

A turbine blade was then considered as a case study due to its complex non-planar shape. In particular, a groove is placed in the middle of the blade (for further testing purposes), and the whole surface is characterized by a relevant curvature. The blade is soldered at the base, representing a cantilever beam having variable cross section. Figure 2 shows the blade during the measurement process, with the speckle pattern sprayed on its surface. The load was applied to the back surface at the top-right corner. Anyway, it was not possible to arrange the accelerometer due to the small sizes of the blade (18 × 43 mm) and the small clearance with respect to its mounting. Moreover, the accelerometer application would influence the measurement results due to the mass-loading effect: this further highlights the advantages of the proposed contact-less setup. Figure 5 shows the point cloud representing the surface reconstruction obtained through the pseudo-stereo vision system. As can be noted, the surface is properly represented, and also the detail of the groove is visible in the acquisitions. Some missing areas were found in correspondence of DIC algorithm failures at the end of the stereo matching task, which were due to light reflections on the target surface. Anyway, most of the component surface was successfully reconstructed. The target object resulted do be much stiffer than the validation specimen, thus its vibration level was found to be lower than 0.01 mm in the frequency range of interest. Anyway, a natural mode of the component was found having a natural frequency of 600 Hz. It was then possible to excite the object in resonance conditions, having a peak in the response. The results obtained with the described 3D DIC system are reported in Fig. 6: Fig. 6(a) represents the x-component of the full field displacement map of the blade (the frame corresponding to the maximum displacement was selected), while Fig. 6(b) shows the magnitude of the displacement over time of the points close to the maximum found in Fig. 6(a) (red box). Since it was not possible to

use an accelerometer to measure the actual blade displacement, the measured signal was overlapped to a synthetic sinusoidal wave having the same amplitude as obtained through NHFA elaboration, for comparison purposes. As can be noted, the sinusoidal wave was properly described by the DIC method, even if the amplitude was lower than 0.01 mm. It is worth noting that the noise level in this acquisition is relevant with respect to the signal amplitude, coherently with the results reported in Fig. 4(b).

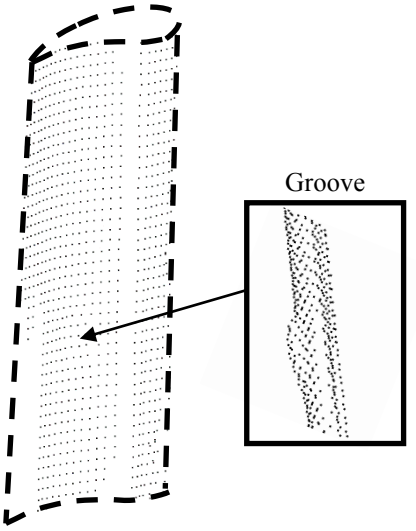

Fig. 5. Point cloud representing the 3D reconstruction of the tested blade.

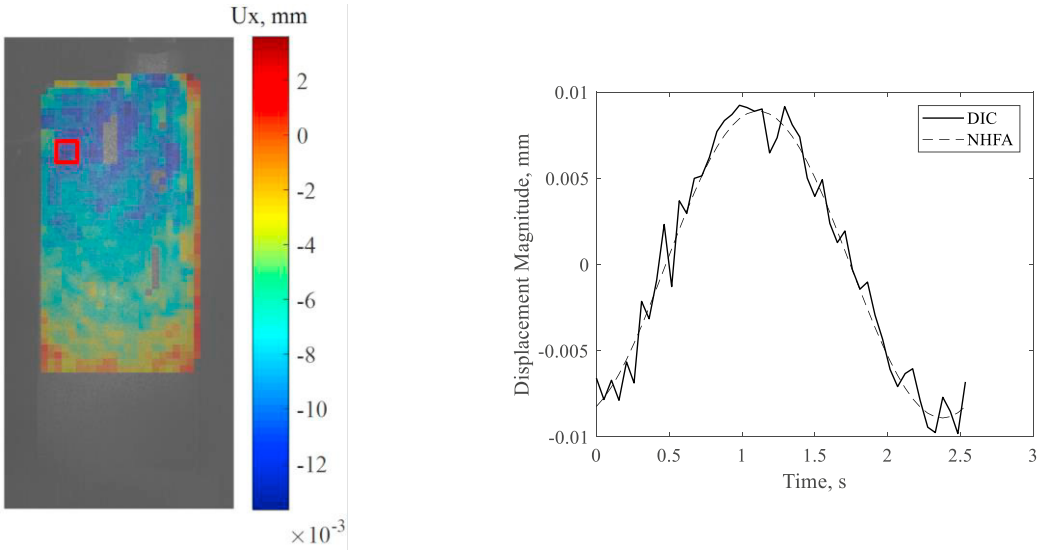

(a) (b)

Fig. 6. DIC results for the turbine blade: (a) full field displacement at maximum deformation and (b) displacement over time of the selected points (red box).

5. Conclusions

In this paper, a single low-speed camera stereo-DIC system has been proposed to carry out 3D full-field vibration measurements up to 1 kHz. The system exploits two planar mirrors and a single low frame rate camera, thus resulting in a compact and low-cost equipment. The effectiveness and accuracy of the proposed approach have been verified

by performing vibration measurements, characterized by a single known frequency component. Firstly, a cantilever plate was simultaneously measured through the proposed DIC setup and an accelerometer. The comparison between these independent amplitude measures allowed to assess the performances of the developed system, which was able to detect a vibration amplitude of 0.01 mm at 920 Hz, with an amplitude error of about 9 %. Finally, the presented DIC system was used for the vibration measurements of a turbine blade: an amplitude of 9 μm was detected at 600 Hz, showing an acceptable noise level. These results allowed to conclude that the proposed low-cost hardware setup based on a single low-frame-rate camera and two planar mirrors represents a reliable tool for high frequency full-field 3D measurements.

Acknowledgements

The authors are grateful to the University of Pisa for supporting this research activity (Grant PRA_2018_80).

References

Barone, S., Neri, P., Paoli, A., Razionale, A., 2017. Digital Image Correlation Based on Projected Pattern for High Frequency Vibration Measurements. Procedia Manufacturing 11, 1592-1599.

Beberniss, T.J., Ehrhardt, D.A., 2017. High-speed 3D digital image correlation vibration measurement: Recent advancements and noted limitations. Mech Syst Signal Pr 86, 35-48.

Bertini, L., Neri, P., Santus, C., Guglielmo, A., 2017. Automated Experimental Modal Analysis of Bladed Wheels with an Anthropomorphic Robotic Station. Exp Mech 57, 273-285.

Bertini, L., Neri, P., Santus, C., Guglielmo, A., Mariotti, G., 2014. Analytical investigation of the SAFE diagram for bladed wheels, numerical and experimental validation. J Sound Vib 333, 4771-4788.

Bouguet, J.Y., 2015. Camera calibration toolbox for Matlab.

Eberl, C., 2010. Digital Image Correlation and Tracking. Mathworks, Matlab Central.

Endo, M.T., Montagnoli, A.N., Nicoletti, R., 2015. Measurement of Shaft Orbits with Photographic Images and Sub-Sampling Technique. Exp Mech 55, 471-481.

Giuliani, P., Di Maio, D., Schwingshackl, C.W., Martarelli, M., Ewins, D.J., 2013. Six degrees of freedom measurement with continuous scanning laser doppler vibrometer. Mech Syst Signal Pr 38, 367-383.

Gluckman, J., Nayar, S.K., 2001. Catadioptric stereo using planar mirrors. Int J Comput Vision 44, 65-79.

Halkon, B.J., Rothberg, S.J., 2006. Vibration measurements using continuous scanning laser vibrometry: Advanced aspects in rotor applications. Mech Syst Signal Pr 20, 1286-1299.

Helfrick, M.N., Niezrecki, C., Avitabile, P., Schmidt, T., 2011. 3D digital image correlation methods for full-field vibration measurement. Mech Syst Signal Pr 25, 917-927.

Kammerer, A., Abhari, R.S., 2009. Experimental Study on Impeller Blade Vibration During Resonance-Part I: Blade Vibration Due to Inlet Flow Distortion. J Eng Gas Turb Power 131.

Lezhin, D.S., Falaleev, S.V., Safin, A.I., Ulanov, A.M., Vergnano, D., 2017. Comparison of different methods of non-contact vibration measurement. Proceedings of the 3rd International Conference on Dynamics and Vibroacoustics of Machines (Dvm2016) 176, 175-183.

Neri, P., 2017. Bladed wheels damage detection through Non -Harmonic Fourier Analysis improved algorithm. Mech Syst Signal Pr 88, 1-8.

Pan, B., Yu, L.P., Zhang, Q.B., 2018. Review of single-camera stereo-digital image correlation techniques for full-field 3D shape and deformation measurement. Sci China Technol Sc 61, 2-20.

Pankow, M., Justusson, B., Waas, A.M., 2010. Three-dimensional digital image correlation technique using single high-speed camera for measuring large out-of-plane displacements at high framing rates. Appl Optics 49, 3418-3427.

Reu, P.L., Rohe, D.P., Jacobs, L.D., 2017. Comparison of DIC and LDV for practical vibration and modal measurements. Mech Syst Signal Pr 86, 2-16.

Sutton, M.A., 2013. Computer Vision-Based, Noncontacting Deformation Measurements in Mechanics: A Generational Transformation. Appl Mech Rev 65.

Yu, L.P., Pan, B., 2017. Single-camera high-speed stereo-digital image correlation for full-field vibration measurement. Mech Syst Signal Pr 94, 374-383.